

See discussions, stats, and author profiles for this publication at: <https://www.researchgate.net/publication/280122395>

# Electrochemical aptamer/antibody based sandwich immunosensor for the detection of EGFR, a cancer biomarker, using gold nanoparticles as a signaling probe

ARTICLE *in* BIOSENSORS & BIOELECTRONICS · JULY 2015

Impact Factor: 6.41 · DOI: 10.1016/j.bios.2015.06.063 · Source: PubMed

---

CITATIONS

2

---

READS

121

## 5 AUTHORS, INCLUDING:



[Hoda Ilkhani](#)

Utah State University

14 PUBLICATIONS 89 CITATIONS

SEE PROFILE



[Abolhassan Noori](#)

Shiraz University

15 PUBLICATIONS 208 CITATIONS

SEE PROFILE



[S. Zahra Bathaie](#)

Tarbiat Modares University

115 PUBLICATIONS 1,233 CITATIONS

SEE PROFILE



[Mir F. Mousavi](#)

Tarbiat Modares University

68 PUBLICATIONS 1,293 CITATIONS

SEE PROFILE



# Electrochemical aptamer/antibody based sandwich immunosensor for the detection of EGFR, a cancer biomarker, using gold nanoparticles as a signaling probe



Hoda Ilkhani<sup>a</sup>, Morteza Sarparast<sup>a</sup>, Abolhassan Noori<sup>a</sup>, S. Zahra Bathaie<sup>b</sup>,  
Mir F. Mousavi<sup>a,\*</sup>

<sup>a</sup> Department of Chemistry, Tarbiat Modares University, Tehran 14115-175, Iran

<sup>b</sup> Department of Clinical Biochemistry, Faculty of Medical Sciences, Tarbiat Modares University, Tehran, Iran

## ARTICLE INFO

### Article history:

Received 10 March 2015

Received in revised form

24 June 2015

Accepted 25 June 2015

Available online 3 July 2015

### Keywords:

EGFR

Electrochemical sandwich immunosensors

Aptamer

Breast cancer

Gold nanoparticles

## ABSTRACT

Detection of epidermal growth factor receptor (EGFR) in biological fluids is of paramount importance, since it has significant application in cancer diagnosis, drug development, and therapy monitoring. EGFR is a cancer biomarker, and its overexpression is associated with the development of some types of cancer. Herein, we report on the development of a sensitive and selective electrochemical aptamer/antibody (Apt/Ab) sandwich immunosensor for detection of EGFR. In this study, a biotinylated anti-human EGFR Apt was immobilized on streptavidin-coated magnetic beads (MB) and served as a capture probe. A polyclonal anti-human EGFR Ab was conjugated to citrate-coated gold nanoparticles (AuNPs) and used as a signaling probe. In the presence of EGFR, an Apt-EGFR-Ab sandwich was formed on the MB surface. The extent of the complexation was evaluated by differential pulse voltammetry of AuNPs after their dissolution in HCl. Under optimal conditions, the dynamic concentration range of the immunosensor for EGFR spanned from 1 to 40 ng/mL, with a low detection limit of 50 pg/mL, and RSD percent of less than 4.2%. The proposed approach takes advantage of sandwich assay for high specificity, MBs for fast separation, and electrochemical method for cost-effective and sensitive detection. In this proof-of-principle study, we demonstrate the potential clinical efficacy of the immunosensor for monitoring of chemotherapy effectiveness in breast cancer samples.

© 2015 Elsevier B.V. All rights reserved.

## 1. Introduction

Epidermal growth factor receptor (EGFR), one of the four members of the ErbB family of tyrosine kinase growth factor receptors, is a cellular trans-membrane protein that is activated through binding to its specific ligands. Activation and auto-phosphorylation of the EGFR initiates a series of intracellular signaling pathways that control critical cell processes such as proliferation, adhesion, migration and apoptosis (Herbst, 2004). Overexpression of EGFR protein has been reported in a wide variety of carcinomas, including breast, head/neck, ovarian, and colorectal cancers (Thomas et al., 2008). The increased EGFR expression has been associated with advanced diseases, development of metastases, and poor clinical outcomes (Aloia et al., 2001; Gibson et al., 2003; Wilkinson et al., 2004). Conventional ways of measuring EGFR as a

cancer biomarker often require sophisticated instrumentation, a specially trained person, protein isolation and clinically unrealistic expense and time (Thariat et al., 2012). Thus, development of a sensitive, simple, fast, and low-cost method for point-of-care cancer biomarker detection is crucial.

Several biosensing strategies have been developed for the detection of EGFR (Chung et al., 2011; Ongarora et al., 2012; Qi et al., 2012, 2009; Yewale et al., 2013; Yuan et al., 2013). The plasmonic gold nanoparticle (AuNP) conjugated to EGFR (Aaron et al., 2009), fluorescent polystyrene nanoparticle conjugated to a monoclonal anti-EGFR antibody (Ab) (Chan et al., 2012), a nano-bio-chip sensor sensitive to EGFR (Weigum et al., 2010), a label free quartz crystal microbalance-based biosensor using anti-EGFR Ab (Chen et al., 2011), and a field-effect transistor-based immunosensor using ZnO thin film (Reyes et al., 2011) are some recently reported studies for the detection of EGFR. In addition, photothermal ablation therapy of epithelial cancer cells using EGFR aptamer (Apt) conjugated to PEGylated gold nanorods has recently been reported (Choi et al., 2014). In most of previous studies the main goal has been addressing upregulated expression of EGFR or studying

\* Corresponding author. Fax: +98 21 82883455.

E-mail addresses: [mfmousavi@yahoo.com](mailto:mfmousavi@yahoo.com),  
[mousavim@modares.ac.ir](mailto:mousavim@modares.ac.ir) (M.F. Mousavi).

therapeutic applicability of the bioconjugate EGFR, whereas very few studies have been dedicated to quantification of EGFR for early-state cancer recognition.

More recently, many research groups have started working on the development of electrochemical techniques as simple, low-cost and sensitive methods for the detection of EGFR (Elshafey et al., 2013; Takahashi et al., 2009, 2011; Vasudev et al., 2013). Electrochemical techniques have partially addressed the drawbacks associated with the other methods. Matsue research group has imaged EGFR on a single living mammalian cell by scanning electrochemical microscopy (Takahashi et al., 2009, 2011). Self-assembly, which has also been a commonly used surface modification technology for studying proteins and other biomolecules (Alizadeh et al., 2013; Hamzehloei et al., 2012; Moradi et al., 2013), has been used for the detection of EGFR (Vasudev et al., 2013).

As indicated above, in most of the EGFR detection approaches, Abs have served as recognition elements. Monoclonal Abs provide a high level of specificity, while polyclonal Abs provide a higher level of sensitivity. However, there is a possibility of cross-reactivity due to a less precisely defined epitope for a polyclonal Ab (Abbaspour et al., 2015). Dissociation constant of Apts, as a class of affinity binding agents, with their target protein is comparable to monoclonal Abs (typically in the range of low micromolar to high picomolar levels), with a high level of specificity, sensitivity, and repeatability (Luo et al., 2013). Apts are small, synthetic molecules that can be produced in a large quantity, with a lower cost, more simplicity and lesser batch-to-batch variation than monoclonal Abs. The combinations of these advantageous properties make Apts an appropriate alternative to Abs (Justino et al., 2015).

MBs as a carrier of affinity complexes (in our case, MB-Apt/EGFR/Ab-AuNP) suit best for the studying of biomolecular interactions (Noori et al., 2010; Reddy et al., 2012). MBs are dispersible in solution, thus MB-Apt conjugates could greatly improve the efficiency of cancer biomarker capturing. The efficiency of bio-recognition reaction in a solution phase is higher than that on a solid substrate. In addition, efficient magnetic separation excludes unwanted constituents from the MB suspension.

Recent advances in nanotechnology and bioconjugated nanomaterials have provided a major expansion in the field of

biosensing, diagnostics, and therapeutic developments. The interest in using nanoparticles (NPs) and nanostructured materials in diverse disciplines arises from their unique size-dependent optical, electrical, and chemical properties (Alizadeh et al., 2011; Ghanbari et al., 2008; Ilkhani et al., 2013). High surface-to-volume ratio of the NPs allows the immobilization of multiple biomolecules on their surface (Mao et al., 2013; Reddy et al., 2012). These exclusive properties stimulate interest in using nanomaterials in new and improved biomedical applications (Abbaspour and Noori, 2012; Elahi et al., 2012).

In this study, a new electrochemical strategy is presented for electrochemical immunosensing of EGFR by using Apt/Ab sandwich assay (Fig. 1). Biotinylated EGFR Apt was immobilized on streptavidin-coated MBs via biotin-streptavidin interaction. AuNPs were synthesized and citrate-coated to provide negatively charged NPs. Polyclonal anti-EGFR Ab was conjugated to AuNPs (Ab-AuNP) and served as a detection probe. When a sample containing EGFR adds to MB-Apt suspension, EGFR is captured via the specific interaction between an Apt and EGFR (biomarker). Then Ab-AuNP is added to the solution, thus completing the sandwich. After that, MBs that are carrying the affinity complex are separated with an external magnet. The detection of EGFR is accomplished by differential pulse voltammetry of the AuNPs after their dissolution in an acidic medium. All of the key parameters that may influence the output signal of the immunosensor are optimized. Finally, the applicability of the immunosensor for the detection of EGFR in serum samples of healthy individuals and women that suffering from (or are suspicious to) breast cancer are evaluated. To the best of our knowledge, this is the first report on an Apt/Ab-based sandwich EGFR immunosensing.

## 2. Experimental

Detailed description on chemicals and reagents, apparatus, and procedures for fabrication of the immunosensor, including synthesis of AuNPs, conjugation of Ab to AuNP, immobilization of the Apt onto MB, optimization of the parameters and electrochemical detection, are given in the Supporting information (see

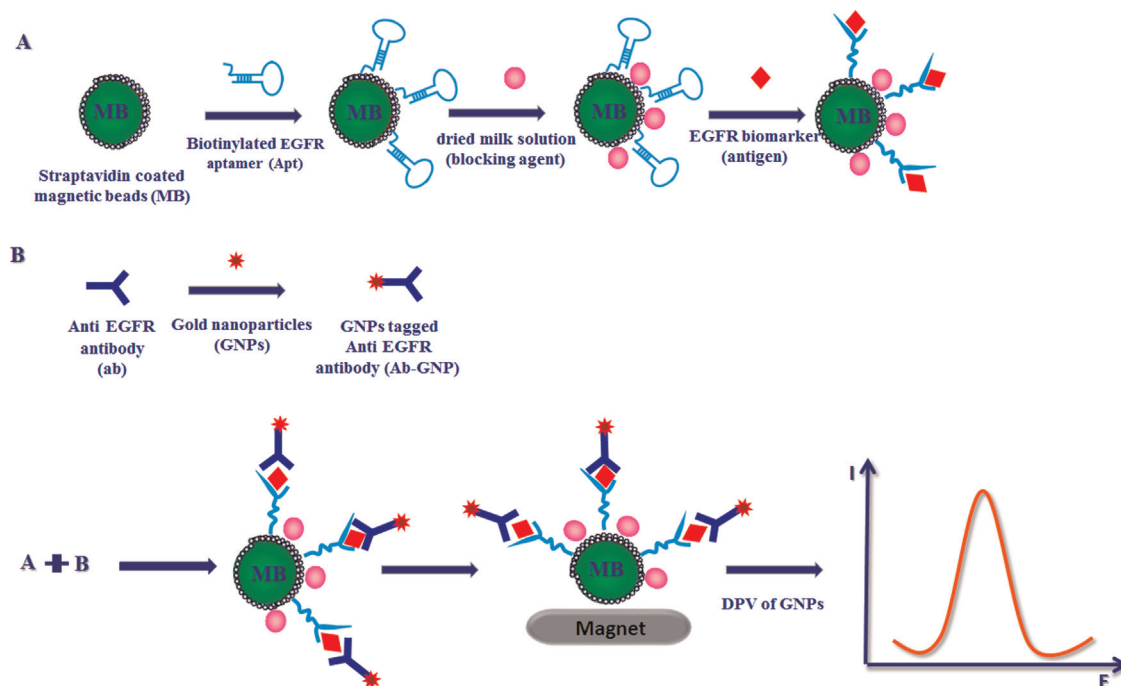


Fig. 1. Schematic representation of the Apt/Ab sandwich assay of EGFR.

SI, Experimental section).

### 3. Results and discussion

#### 3.1. Characterization of AuNPs

Citrate-coated AuNPs were synthesized based on an established procedure (Frens, 1973). To characterize AuNPs, UV–vis absorption spectrum (Fig. 2A curve a) and transmission electron microscopy (TEM) image (Fig. 2B) of the AuNPs suspension were obtained. The AuNPs are plasmonic nanoparticles that are highly efficient at absorbing and scattering the light. The origin of the unique spectral response of the AuNPs is the resonant oscillation of conduction electrons with specific wavelengths of light, a phenomenon known as a surface plasmon resonance. The AuNPs suspension shows a plasmon absorption band at 525 nm. The relative percentage of absorbing or scattering the light depends on the size, shape, composition, and aggregation state of the AuNPs sample. Most of the AuNPs samples have contributions from both absorption and scattering. The dependence of the optical properties of the AuNPs to particle size and wavelength has been analyzed using the multipole scattering theory (Haiss et al., 2007). Previous studies have shown an excellent agreement between theoretical and experimental results for the size evaluation of the AuNPs in the range of 5–100 nm. We used the same procedure for determination of both the size and concentration of the AuNPs directly from UV–vis spectra. The size of nanoparticles was calculated as 32 nm using multipole scattering theory and the concentration of the AuNPs was calculated as 0.268  $\mu\text{g/mL}$  (see SI, determination of size and concentration of the AuNPs from UV–vis spectrum). TEM image of the AuNPs shows that the AuNPs with uniform size distribution are synthesized. The size of AuNPs was approximately 30 nm, which is consistent with that obtained by theoretical method (Fig. 2B).

#### 3.2. Conjugation of anti-EGFR Ab to AuNPs

For characterization of the conjugation of Ab to AuNPs, UV–vis absorption spectrum of AuNPs after conjugation with Ab was recorded. As is presented in Fig. 2A curve b, the absorption spectrum of Ab–AuNPs shows a characteristic red-shift of the plasmon absorption peak (about 5 nm) compared to the colloid AuNPs suspension at 525 nm, which indicates the difference in the dielectric

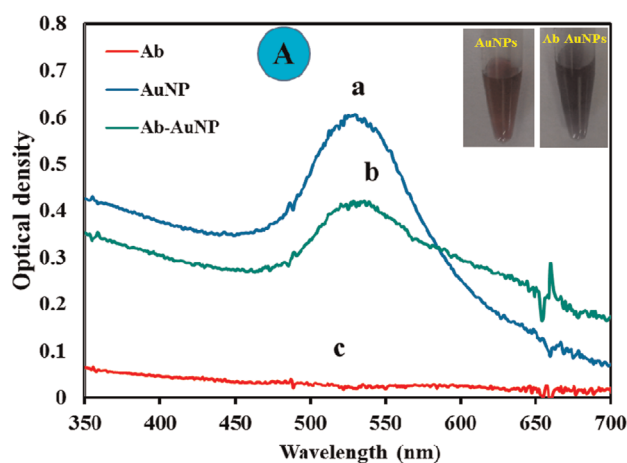


**Fig. 2.** (A) UV–vis absorption spectra of (a) AuNPs, (b) Ab-conjugated AuNPs and (c) Ab. The inset photograph shows the change in color of the AuNP suspension from red to purple after Ab conjugation. (B) TEM image of AuNPs. The inset presents the image with a higher magnification. (For interpretation of the references to color in this figure legend, the reader is referred to the web version of this article.)

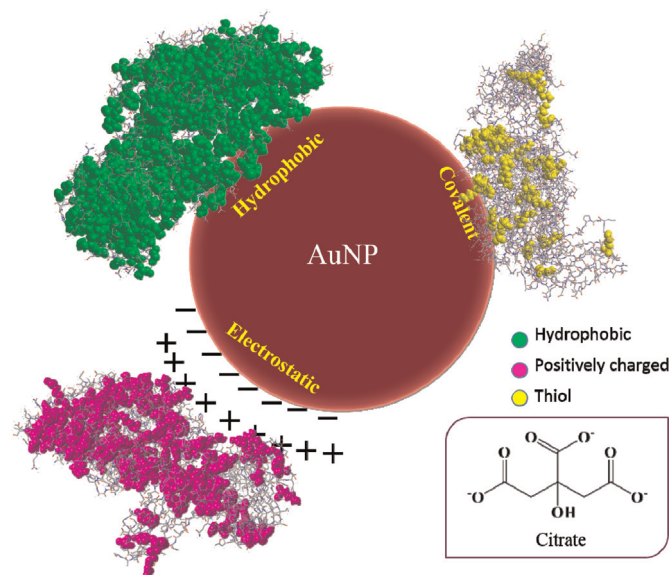
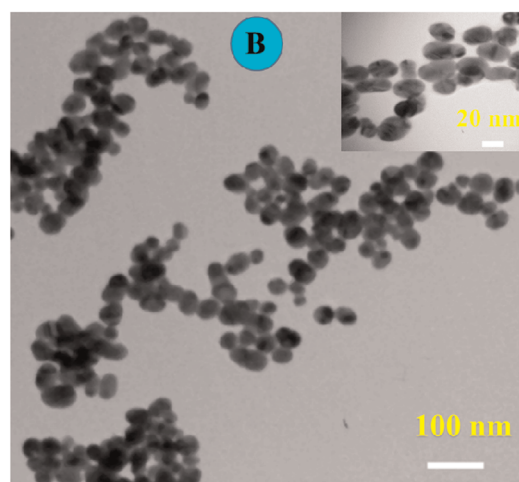


**Fig. 3.** Schematic representation of the different modes of interaction involved in conjugation of Abs to AuNPs.

environment of AuNP before and after binding to and conjugation with anti-EGFR Ab (Joshi et al., 2013). This conjugation is also accompanied by a decrease in peak intensities and broadening of absorption peaks. This observation is also consistent with the literature, indicating the inter-particle interactions and formation of some agglomerates (Willems and Van Duyn, 2007). To go through the detailed description of the course of Ab–AuNPs conjugation, please see Fig. 3 and SI file, strategies for AuNPs bioconjugation. The conjugation of the Ab to AuNPs is also visually detectable with a change in the color of solution from red to purple (Fig. 2A, inset).

#### 3.3. Optimized parameters

In a common sandwich assay several parameters are of critical importance, and the optimal condition for target recognition of one Ab may not be the same for another. Herein, we have started with standard conditions as a starting point and then optimized the concentrations of Apt, Ab and blocking agent, as well as all the incubation times to achieve the highest signal-to-noise ratio of the electrochemical signal. These factors all influence the ultimate





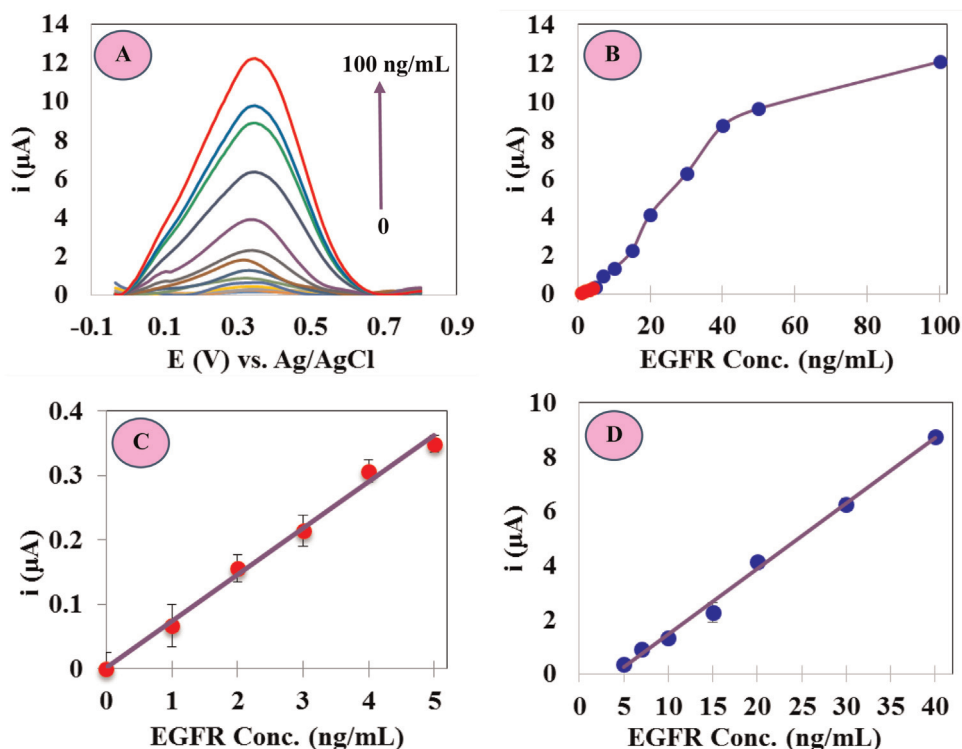


**Fig. 4.** (A) Background-subtracted DPVs of different concentrations of EGFR biomarker in the range of 1–40 ng/mL. (B) Plot of EGFR concentration (in the range of 1–100 ng/mL) versus oxidation peak current of the AuNPs. (C) Calibration curve for quantification of EGFR in the range of 1–5 ng/mL, and (D) Calibration curve for quantification of EGFR in the range of 5–40 ng/mL. The points and error bars correspond to the mean  $\pm$  standard deviation of three repetitions.

selectivity and sensitivity of the immunosensor. For the detailed description of the optimization steps and the results please note to SI file, optimization of parameters.

### 3.4. Analytical application

Under the optimized conditions described above, the electrochemical response of the immunosensor was recorded as a function of EGFR concentration (Fig. 4A). Electrochemical response of the immunosensor increased with increasing the EGFR concentration. Fig. 4B shows the plot of DPV peak current versus EGFR concentration in the range of 1–100 ng/mL. At concentrations higher than 40 ng/mL, the signal of the immunosensor leveled off. Each voltammogram is the average of three repetitive measurement, and the standard deviation of the three measurement provides a metric to evaluate the repeatability of the biosensor. As is shown in Fig. 4B, electrochemical signal of the immunosensor at lower concentrations of EGFR rises less steeply than that at higher concentrations of EGFR. Fig. 4B indicates that the data of the full range of the EGFR concentration, from 1 to 40 ng/mL, do not fit with a single linear regression equation. Different mathematical functions including logarithmic, exponential, power, and segmented linear functions are used in the field of nonlinear regression. Among all, power function and segmented linear regression model, consisting of two linear segments, described the detection system significantly better than the other regression models (see SI, regression equations and Figure S9). Linear regression functions are more convenient, and one can obtain very good results with relatively small data sets. Thus, among all, we have used a segmented linear function to relate the analytical signal of the immunosensor to EGFR concentration. The first linear segment (Fig. 4C) expands from 1 to 5 ng/mL with a linear regression equation of  $I (\mu\text{A}) = 0.0722C_{\text{EGFR}} (\text{ng/mL}) + 0.0017$  ( $R^2 = 0.993$ ) and the second linear segment (Fig. 4D) extends from 5.0 to 40.0 ng/mL with a linear regression equation of  $I (\mu\text{A}) =$

$$0.2417C_{\text{EGFR}} (\text{ng/mL}) - 0.9597 \quad (R^2 = 0.995).$$

Limit of detection (LOD) of the assay (based on the regression equation of first linear segment) was 50 pg/mL, which was more sensitive than that of the commercial EGFR ELISA kit (300 ng/mL, human EGFR full length ELISA Kit, Invitrogen, USA). The sensitivity of the biosensor, was also considerably better than or comparable to the methods presented for quantification of ErbB growth factor receptors in real clinical samples (Table 1). The boosted electrochemical signal and sensitivity of the immunosensor is largely attributed to the increasing number of gold atoms that are responsible for producing the electrochemical signal, whereas, in most of the signal transduction strategies just a single enzyme, redox probe, or fluorophore is responsible for transduction of the biorecognition reaction into a read-out signal. Moreover, with well-known biotin-streptavidin reactions, as the strongest known non-covalent interaction ( $K_f = 10^{15} \text{ M}^{-1}$ ), one can easily immobilize ligands to MBs surface. In addition, several key advantageous properties of Apts over Abs such as: much easier and more economical production, easy chemical modification to yield improved and tailored properties, improved transport properties while immobilized on MBs, much more stability and shelf-life at ambient temperature, not being aggregated and better tolerating pH and temperature change, make the proposed approach potentially suitable for future clinical applications (Keefe et al., 2010; Wengerter et al., 2014). The Apt that has been used as a capture probe in this study has a high binding constant to the target protein ( $K_d = 2.4 \text{ nM}$ ) (Wan et al., 2013, 2012).

The range of EGFR biomarker in healthy individuals is in the range of about 1.0–25 ng/mL. Its range between primary diagnostic step and metastatic diagnostic step is from about 11–30 ng/mL and in women with breast cancer is up to 270 ng/mL (Kumar et al., 2001). The proposed immunosensor (dynamic range: 1–40 ng/mL) covers just the critical concentration range of the EGFR in serum samples. Thus the limited dynamic range of the immunosensor prevents full exploitation of the proposed approach for the breast

**Table 1**

Comparing the performance of present work with some other assays.

	Method	Assay protocol	Dynamic range	Detection limit	Ref.
1	Voltammetry	Ab immobilized on a SAM modified gold electrode	1 pg/mL–100 ng/mL	1 pg/mL	(Vasudev et al., 2013)
2	Amperometry	Sandwich immunosensor using Abs on MB	0.1–32 ng/mL	26 pg/mL	(Eletxigerra et al., 2015)
3	FRET <sup>a</sup>	QD <sup>b</sup> -based FRET immunoassay	–	23 ng/mL	(Wegner et al., 2014)
4	Capacitive	Using AuNPs for signal enhancement	20–1000 pg/mL	20 pg/mL	(Altintas et al., 2014)
5	LSV <sup>c</sup>	Sandwich immunoassay using two monoclonal Abs	15–100 ng/mL	4.4 ng/mL	(Marques et al., 2014)
6	Impedimetry	Ab/Protein G/1,4-phenylene diisothiocyanate/cysteamine /AuNPs/Au	1 pg/mL–1 µg/mL	0.34 pg/mL	(Elshafey et al., 2013)
7	SERS <sup>d</sup>	PCF <sup>e</sup> -based SERS by using AuNP-conjugated Ab	–	5 ng/mL	(Dinish et al., 2012)
8	Gravimetry	Anti-EGFR Ab immobilized on a gold QCM <sup>f</sup> electrode	0.01–10 µg/mL	100 ng/mL	(Chen et al., 2011)
9	ASDPV <sup>g</sup>	Apt/Ab-based Sandwich immunoassay	1–40 ng/mL	50 pg/mL	This work

<sup>a</sup> Förster resonance energy transfer.<sup>b</sup> Quantum dots.<sup>c</sup> Linear sweep voltammetry.<sup>d</sup> Surface enhanced Raman scattering.<sup>e</sup> Photonic crystal fiber.<sup>f</sup> Quartz crystal microbalance.<sup>g</sup> Anodic stripping differential pulse voltammetry.

cancer detection, and further improvements are required to make the detection method a state of the art approach for real time EGFR quantification. However, for precise quantification of EGFR in serum samples from women with breast cancer, the sample can be diluted till the level of EGFR falls within the dynamic range of the immunosensor. Although limited dynamic range is a potential drawback for the system (that impedes the applicability of the immunosensor for direct in-vivo analyses), there exists enormous potential for an electrochemical detection approach that can compensate for its shortcoming. Ricci research group have demonstrated a method to extend or narrow the useful dynamic range of a model electrochemical DNA sensor (Kang et al. 2012). They have co-immobilized DNA probes of different target affinities but with similar specificity on an electrode, and tuned the dynamic range of the sensor spanning 8-fold to 3 orders of magnitude. Since Apts are DNA molecules, immobilization of EGFR Apts, that are specific to EGFR but with different affinities, would provide a potential solution for tuning the dynamic range of the immunosensor. Potential miniaturization of electrochemical detection and interrogation of Apts on microarray platform results in a high-throughput analysis that allowing parallel implementation of thousands of experiments that can appropriately compensate for some limitations of the method in real-world biomedical applications.

The repeatability of the biosensor was evaluated from the relative standard deviation (RSD) of three different measurements of 4.0 and 30.0 ng/mL EGFR solutions with the same biosensor. RSD values of 4.23% and 3.28% were obtained, respectively. The storage stability of the biosensor was studied by storing the Apt-immobilized MB in a refrigerator at 4 °C. The biosensor retained more than 95% of the initial response after 7 days, indicating the desirable stability of the biosensor. The analytical characteristics of the present study were compared to the previously reported methods with the same detection strategy. Marques et al. have reported an electrochemical EGFR biosensor in which a screen printed graphite electrode has been modified with AuNPs and two monoclonal Abs were used to establish a sandwich assay (Marques et al., 2014; Li et al., 2013). The sensor has responded linearly to EGFR concentration in the range of 15–100 ng/mL with a detection limit of 4.4 ng/mL. Thus, it can be deduced that the use of an Apt as a capture probe instead of an Ab improves the detection sensitivity of the immunosensor. In another analogs approach, a sandwich immunosensor using Abs (one immobilized on MBs as a capture probe and another conjugated to an enzyme as a reporter), with amperometric detection method, has provided detection limit of 26 pg/mL (Eletxigerra et al., 2015). Table 1 presents a comparison

of the present study with previous works. Comparing the characteristics of the present study with other methods indicates suitability of the work for sensitive detection of EGFR. However, some of the works in this collection present an enormously extended dynamic range (e.g. Elshafey et al., 2013). In that approach, Elshafey et al. have covalently conjugated a protein and other intermediates on an electrode surface, which has been a more sophisticated and multi-step process. Although sandwich assay is also a multistep process, we have used an affinity based biorecognition reaction (as a non-covalent but extremely stable bond that resists harsh chemical conditions) that simplifies and more generalizes the detection method.

### 3.5. Serum specimen analysis

Because of the use of the EGFR-specific Ab and Apt, sandwich assay method allowed us to quantify EGFR without interference from other substrates in real samples. Once verified the suitability of the assay for the detection of EGFR in standard solutions, preliminary experiments were carried out on serum samples. For this goal, batches of blood serums from healthy females with very low (< 2 ng/mL) EGFR contents were spiked with EGFR in order to have six different final concentrations in the range of 4–30 ng/mL. Each spiked sample was filtered and then diluted 1:2 before incubation with functionalized MBs. The results show a good agreement between the spiked and obtained values of EGFR in serum samples of healthy individuals (Table 2). The recovery values are close to 100%, confirming that the performance of the biosensor has not been affected by the nature of the serum samples. The higher recovery value of the sample spiked with 4 ng/mL EGFR (112.3%) can be attributed to the contribution of EGFR biomarkers that are present in serum samples of healthy individuals. Reproducibility of this immunosensor is comparable to that found in standard solutions, thus confirms the suitability of the proposed

**Table 2**Spike and recovery results ( $n=3$ ) obtained from the fabricated EGFR immunosensor in serum samples.

Sample no.	Spiked (ng/mL)	Obtained <sup>a</sup> (ng/mL)	Recovery (%)
1	4	4.49 ± 0.05	112.3
2	6	5.38 ± 0.04	89.7
3	12	11.26 ± 0.31	93.8
4	19	19.18 ± 0.24	100.9
5	23	24.71 ± 0.18	107.4
6	30	29.26 ± 0.21	97.5

<sup>a</sup> Mean ± standard deviation,  $n=3$ .

approach for real sample analyses. However, the interference of some species (that may have an abnormally high concentrations in some serums samples) has not been tested. It could be a possible challenge, and should be taken into account for future development of the assay.

In the next step, analyses of clinical real samples continued with analyzing serums of healthy individuals (6 samples) and breast cancer patients under chemotherapy (3 samples). The EGFR concentrations in the serum samples of healthy individuals, measured using the proposed immunosensor, were less than 3 ng/ml, and for those with breast cancer estimated to be more than 40 ng/mL. Thus, the sensor can successfully discriminate between healthy and cancerous samples. We anticipate that this proof-of-principle study will be a basis for the future development of new potential strategies to monitor the progression of the disease and effectiveness of treatment of breast cancer patients by sensitive and specific EGFR targeting in an extended dynamic range.

However, it should be emphasized that EGFR is not a specific breast cancer biomarker. Thus, the high level of EGFR in a serum sample cannot be confidently associated with breast cancer. As mentioned above, The EGFR overexpression have been reported in other types of cancer such as lung, head/neck and ovarian cancers, as well as anal squamous intraepithelial lesions (Walker et al., 2009; Jost et al., 2000). But in clinical diagnosis, there is a continuous need for a simple, miniaturizable, portable, sensitive and cheap method of detection. Here, we propose an approach for quantification of EGFR in clinical real samples, which has the potential to be applied for the detection of different cancers. This study is continuing, and further work is necessary to design and establish a sophisticated protocols for cancer prediction with EGFR detection.

#### 4. Conclusion

In this study, for the first time, an electrochemical Apt/Ab sandwich assay is designed for EGFR detection. Application of an Apt as a capture probe, with comparable characteristics to conventional monoclonal Abs, but with much lower cost and easy modification capability increased the robustness and applicability of the immunosensor. Ab was conjugated to the AuNP as a detection probe that provided an acceptable level of sensitivity for the detection of EGFR as a cancer biomarker. Preliminary results of the immunosensor for quantification of EGFR in serum samples are presented here. Although still in the proof-of-concept stage, the proposed approach may promote the future design and development of a more sensitive immunosensor for precise quantification of EGFR biomarker in complex biological samples.

#### Author's contribution

H.I., M.S. and A.N. contributed equally to this work.

#### Acknowledgment

Financial supports of the work by Tarbiat Modares University Research Council and Iranian National Science Foundation (INSF) (Grant number 91049974) are highly acknowledged.

#### Appendix A. Supplementary material

Supplementary data associated with this article can be found in the online version at <http://dx.doi.org/10.1016/j.bios.2015.06.063>.

#### References

- Aaron, J., Travis, K., Harrison, N., Sokolov, K., 2009. Dynamic imaging of molecular assemblies in live cells based on nanoparticle plasmon resonance coupling. *Nano Lett.* 9 (10), 3612–3618.
- Abbaspour, A., Noori, A., 2012. Electrochemical detection of individual single nucleotide polymorphisms using monobase-modified apoferritin-encapsulated nanoparticles. *Biosens. Bioelectron.* 37 (1), 11–18.
- Abbaspour, A., Norouz-Sarvestani, F., Noori, A., Soltani, N., 2015. Aptamer-conjugated silver nanoparticles for electrochemical dual-Aptamer-based sandwich detection of staphylococcus aureus. *Biosens. Bioelectron.* 68 (0), 149–155.
- Alizadeh, V., Mehrgardi, M.A., Mousavi, M.F., 2013. Electrochemical investigation of cytochrome c immobilized onto self-assembled monolayer of captopril. *Electroanalysis* 25 (7), 1689–1696.
- Alizadeh, V., Mousavi, M.F., Mehrgardi, M.A., Kazemi, S.H., Sharghi, H., 2011. Electron transfer kinetics of cytochrome c immobilized on a phenolic terminated thiol self assembled monolayer determined by scanning electrochemical microscopy. *Electrochim. Acta* 56 (17), 6224–6229.
- Aloia, T.A., H.D.J., Reed, C.E., Allegra, C., Moore, M.B., Herndon 2nd, J.E., D'Amico, T. A., 2001. Tumor marker expression is predictive of survival in patients with esophageal cancer. *Ann. Thorac. Surg.* 72, 3.
- Altintas, Z., Kallemudi, S.S., Gurbuz, Y., 2014. Gold nanoparticle modified capacitive sensor platform for multiple marker detection. *Talanta* 118, 270–276.
- Chan, L.W., Wang, Y.N., Lin, L.Y., Upton, M.P., Hwang, J.H., Pun, S.H., 2012. Synthesis and characterization of anti-egfr fluorescent nanoparticles for optical molecular imaging. *Bioconjug. Chem.* 24 (2), 167–175.
- Chen, J.C., Sadhasivam, S., Lin, F.H., 2011. Label free gravimetric detection of epidermal growth factor receptor by antibody immobilization on quartz crystal microbalance. *Process Biochem.* 46 (2), 543–550.
- Choi, J., Park, Y., Choi, E.B., Kim, H.O., Kim, D.J., Hong, Y., Ryu, S.H., Lee, J.H., Suh, J.S., Yang, J., Huh, Y.M., Haam, S., 2014. Aptamer-conjugated gold nanorod for photothermal ablation of epidermal growth factor receptor-overexpressed epithelial cancer. *J. Biomed. Opt.* 19, 5.
- Chung, T.H., Hsiao, J.K., Hsu, S.C., Yao, M., Chen, Y.C., Wang, S.W., Kuo, M.Y.P., Yang, C. S., Huang, D.M., 2011. Iron oxide nanoparticle-induced epidermal growth factor receptor expression in human stem cells for tumor therapy. *ACS Nano* 5 (12), 9807–9816.
- Dinish, U.S., Fu, C.Y., Soh, K.S., Ramaswamy, B., Kumar, A., Olivo, M., 2012. Highly sensitive SERS detection of cancer proteins in low sample volume using hollow core photonic crystal fiber. *Biosens. Bioelectron.* 33 (1), 293–298.
- Elahi, M.Y., Bathaie, S.Z., Mousavi, M.F., Hoshyar, R., Ghasemi, S., 2012. A new DNA-nanobiosensor based on G-quadruplex immobilized on carbon nanotubes modified glassy carbon electrode. *Electrochim. Acta* 82 (0), 143–151.
- Eletxigerra, U., Martinez-Perdiguero, J., Merino, S., Barderas, R., Torrente-Rodríguez, R.M., Villalonga, R., Pingarrón, J.M., Campuzano, S., 2015. Amperometric magnetosensory detection of ErbB2 breast cancer biomarker determination in human serum, cell lysates and intact breast cancer cells. *Biosens. Bioelectron.* 70 (0), 34–41.
- Elshafey, R., Tavares, A.C., Sijaj, M., Zourob, M., 2013. Electrochemical impedance immunosensor based on gold nanoparticles-protein G for the detection of cancer marker epidermal growth factor receptor in human plasma and brain tissue. *Biosens. Bioelectron.* 50, 143–149.
- Frens, G., 1973. Controlled nucleation for the regulation of the particle size in monodisperse gold suspensions. *Nat. Phys. Sci.* 241 (105), 20–22.
- Ghanbari, K., Bathaie, S.Z., Mousavi, M.F., 2008. Electrochemically fabricated polypyrrole nanofiber-modified electrode as a new electrochemical DNA biosensor. *Biosens. Bioelectron.* 23 (12), 1825–1831.
- Gibson, M.K., Abraham, S.C., Wu, T.T., Burtness, B., Heitmiller, R.F., Heath, E., Forastiere, A., 2003. Epidermal growth factor receptor, p53 mutation, and pathological response predict survival in patients with locally advanced esophageal cancer treated with preoperative chemoradiotherapy. *Clin. Cancer Res.: Off. J. Am. Assoc. Cancer Res.* 9 (17), 6461–6468.
- Haiss, W., Thanh, N.T.K., Aveyard, J., Fernig, D.G., 2007. Determination of size and concentration of gold nanoparticles from UV–vis spectra. *Anal. Chem.* 79 (11), 4215–4221.
- Hamzehloei, A., Mousavi, M.F., Bathaie, S.Z., 2012. In Situ synthesis of a novel quinone imine self-assembled monolayer and consideration of its reactivity with L-arginine. *Electroanalysis* 24 (6), 1362–1373.
- Herbst, R.S., 2004. Review of epidermal growth factor receptor biology. *Int. J. Radiat. Oncol. Biol. Phys.* 59 (2 Suppl), 21–26.
- Ilkhani, H., Arvand, M., Ganjali, M.R., Marrazza, G., Mascini, M., 2013. Nanostructured screen printed graphite electrode for the development of a novel electrochemical genosensor. *Electroanalysis* 25 (2), 507–514.
- Joshi, P.P., Yoon, S.J., Hardin, W.G., Emelianov, S., Sokolov, K.V., 2013. Conjugation of antibodies to gold nanorods through Fc portion: synthesis and molecular specific imaging. *Bioconjug. Chem.* 24 (6), 878–888.
- Jost, M., Kari, C., Rodeck, U., 2000. The EGF receptor—an essential regulator of multiple epidermal functions. *Eur. J. Dermatol.: EJD* 10 (7), 505–510.
- Justino, C.I.L., Freitas, A.C., Pereira, R., Duarte, A.C., Rocha Santos, T.A.P., 2015. Recent developments in recognition elements for chemical sensors and biosensors. *TrAC Trends Anal. Chem.* 68 (0), 2–17.
- Keefe, A.D., Pai, S., Ellington, A., 2010. Aptamers as therapeutics. *Nat. Rev. Drug Discov.* 9 (7), 537–550.
- Kumar, R.R., Meenakshi, A., Sivakumar, N., 2001. Enzyme immunoassay of human epidermal growth factor receptor (hEGFR). *Hum. Antib.* 10 (3), 143–147.

- Li, R., Huang, H., Huang, L., Lin, Z., Guo, L., Qiu, B., Chen, G., 2013. Electrochemical biosensor for epidermal growth factor receptor detection with peptide ligand. *Electrochim. Acta* 109 (0), 233–237.
- Luo, Y., Liu, X., Jiang, T., Liao, P., Fu, W., 2013. Dual-aptamer-based biosensing of toxoplasma antibody. *Anal. Chem.* 85 (17), 8354–8360.
- Mao, H.Y., Laurent, S., Chen, W., Akhavan, O., Imani, M., Ashkarran, A.A., Mahmoudi, M., 2013. Graphene: promises, facts, opportunities, and challenges in nanomedicine. *Chem. Rev.* 113 (5), 3407–3424.
- Marques, R.C.B., Viswanathan, S., Nouws, H.P.A., Delerue-Matos, C., González-García, M.B., 2014. Electrochemical immunosensor for the analysis of the breast cancer biomarker HER2 ECD. *Talanta* 129 (0), 594–599.
- Moradi, N., Mousavi, M.F., Mehrgardi, M.A., Noori, A., 2013. Preparation of a new electrochemical biosensor for single base mismatch detection in DNA. *Anal. Methods* 5 (22), 6531–6538.
- Noori, A., Centi, S., Tombelli, S., Mascini, M., 2010. Detection of activated protein C by an electrochemical aptamer-based sandwich assay. *Anal. Bioanal. Electrochem.* 2, 178–188.
- Ongarora, B.G., Fontenot, K.R., Hu, X., Sehgal, I., Satyanarayana-Jois, S.D., Vicente, M. G.H., 2012. Phthalocyanine–peptide conjugates for epidermal growth factor receptor targeting. *J. Med. Chem.* 55 (8), 3725–3738.
- Qi, S., Miao, Z., Liu, H., Xu, Y., Feng, Y., Cheng, Z., 2012. Evaluation of four affibody-based near-infrared fluorescent probes for optical imaging of epidermal growth factor receptor positive tumors. *Bioconjug. Chem.* 23 (6), 1149–1156.
- Qiu, C., Tarrant, M.K., Boronina, T., Longo, P.A., Kavran, J.M., Cole, R.N., Cole, P.A., Leahy, D.J., 2009. In vitro enzymatic characterization of near full length egfr in activated and inhibited states. *Biochemistry* 48 (28), 6624–6632.
- Reddy, L.H., Arias, J.L., Nicolas, J., Couvreur, P., 2012. Magnetic nanoparticles: Design and characterization, toxicity and biocompatibility, pharmaceutical and biomedical applications. *Chem. Rev.* 112 (11), 5818–5878.
- Reyes, P.I., Ku, C.J., Duan, Z., Lu, Y., Solanki, A., Lee, K.B., 2011. ZnO thin film transistor immunosensor with high sensitivity and selectivity. *Appl. Phys. Lett.* 98 (17), 173702–173703.
- Takahashi, Y., Miyamoto, T., Shiku, H., Asano, R., Yasukawa, T., Kumagai, I., Matsue, T., 2009. Electrochemical detection of epidermal growth factor receptors on a single living cell surface by scanning electrochemical microscopy. *Anal. Chem.* 81 (7), 2785–2790.
- Takahashi, Y., Miyamoto, T., Shiku, H., Ino, K., Yasukawa, T., Asano, R., Kumagai, I., Matsue, T., 2011. Electrochemical detection of receptor-mediated endocytosis by scanning electrochemical microscopy. *Phys. Chem. Chem. Phys.* 13 (37), 16569–16573.
- Thariat, J., Etienne-Grimaldi, M.C., Grall, D., Bensadoun, R.-J., Cayre, A., Penault-Llorca, F., Veracini, L., Francoual, M., Formento, J.L., Dassonville, O., De Raucourt, D., Geoffrois, L., Giraud, P., Racadot, S., Morinière, S., Milano, G., Van Obberghen-Schilling, E., 2012. Epidermal growth factor receptor protein detection in head and neck cancer patients: a many-faceted picture. *Clin. Cancer Res.* 18 (5), 1313–1322.
- Thomas, T.P., Shukla, R., Kotlyar, A., Liang, B., Ye, J.Y., Norris, T.B., Baker, J.R., 2008. Dendrimer – epidermal growth factor conjugate displays superagonist activity. *Biomacromolecules* 9 (2), 603–609.
- Vasudev, A., Kaushik, A., Bhansali, S., 2013. Electrochemical immunosensor for label free epidermal growth factor receptor (EGFR) detection. *Biosens. Bioelectron.* 39 (1), 300–305.
- Walker, F., Abramowitz, L., Benabderrahmane, D., Duval, X., Descatoire, V., Hénin, D., Lehy, T., Aparicio, T., 2009. Growth factor receptor expression in anal squamous lesions: modifications associated with oncogenic human papillomavirus and human immunodeficiency virus. *Hum. Pathol.* 40 (11), 1517–1527.
- Wan, Y., Mahmood, M.A.I., Li, N., Allen, P.B., Kim, Y.T., Bachoo, R., Ellington, A.D., Iqbal, S.M., 2012. Nanotextured substrates with immobilized aptamers for cancer cell isolation and cytology. *Cancer* 118 (4), 1145–1154.
- Wan, Y., Tamuly, D., Allen, P.B., Kim, Y.T., Bachoo, R., Ellington, A.D., Iqbal, S.M., 2013. Proliferation and migration of tumor cells in tapered channels. *Biomed. Microdevices* 15 (4), 635–643.
- Wegner, K.D., Lindén, S., Jin, Z., Jennings, L.T., el Khoulati, R., Henegouwen, P.M.P.B., Hildebrandt, N., 2014. Nanobodies and Nanocrystals: Highly Sensitive Quantum Dot-Based Homogeneous FRET Immunoassay for Serum-Based EGFR Detection. *Small* 10 (4), 734–740.
- Weigum, S.E., Floriano, P.N., Redding, S.W., Yeh, C.-K., Westbrook, S.D., McGuff, H.S., Lin, A., Miller, F.R., Villarreal, F., Rowan, S.D., Vigneswaran, N., Williams, M.D., McDevitt, J.T., 2010. Nano-bio-chip sensor platform for examination of oral exfoliative cytology. *Cancer Prev. Res.* 3 (4), 518–528.
- Wengerter, B.C., Katakowski, J.A., Rosenberg, J.M., Park, C.G., Almo, S.C., Palliser, D., Levy, M., 2014. Aptamer-targeted antigen delivery. *Mol. Ther.* 22 (7), 1375–1387.
- Wilkinson, N., Black, J.D., Roukhadze, E., Driscoll, D., Smiley, S., Hoshi, H., Geradts, J., Javle, M., Brattain, M., 2004. Epidermal growth factor receptor expression correlates with histologic grade in resected esophageal adenocarcinoma. *J. Gastrointest. Surg.* 8 (4), 448–453.
- Willems, K.A., Van Duyne, R.P., 2007. Localized surface plasmon resonance spectroscopy and sensing. *Annu. Rev. Phys. Chem.* 58 (1), 267–297.
- Yewale, C., Baradia, D., Vhora, I., Patil, S., Misra, A., 2013. Epidermal growth factor receptor targeting in cancer: a review of trends and strategies. *Biomaterials* 34 (34), 8690–8707.
- Yuan, Y., Chen, S., Paunesku, T., Gleber, S.C., Liu, W.C., Doty, C.B., Mak, R., Deng, J., Jin, Q., Lai, B., Brister, K., Flachenecker, C., Jacobsen, C., Vogt, S., Woloschak, G.E., 2013. Epidermal growth factor receptor targeted nuclear delivery and high-resolution whole cell X-ray imaging of Fe<sub>3</sub>O<sub>4</sub>@TiO<sub>2</sub> nanoparticles in cancer cells. *ACS Nano* 7 (12), 10502–10517.